

Supporting Information

Xie et al. 10.1073/pnas.1607980113

SI Materials and Methods

Materials. The dense boron carbide was consolidated using spark plasma sintering at 1,900 °C for 5 min. The stoichiometry was measured to be B₄C by X-ray diffraction, Raman spectroscopy, and electron energy loss spectroscopy.

Boron carbide rods with 1×1 -mm² cross-sections were obtained by slicing the dense sample using a diamond saw. Needle-shaped tips were produced by electropolishing the rods in 5% (mass/mass) KOH–water solution. The final shaping was carried out in an FIB (FIB Zeiss; Auriga), milled at 30 keV, and cleaned at 5 keV.

Atom Probe Experiments. Atom probe experiments use the principles of field evaporation. Under a very intense electric field, surface atoms or molecules at the tip of a specimen are polarized, and high-energy voltage pulses can be used to field evaporate individual atoms from conducting metals and alloy specimens. These atoms are ionized during the evaporation process, accelerated by the intense electric field, and recorded by a detector that determines their spatial and chemical identities (Fig. S1). The traditional pulsed voltage approach has also been used to study some semiconductors, but only those with very small band gaps (e.g., highly doped Si) (30). Semiconductors, such as pure Si (room temperature band gap 1.12 eV), are known to be very difficult to field evaporate with voltage pulses. Being a semiconductor, we first attempted to field evaporate our boron carbide specimens using the pulsed voltage technique, but no signal was detected up to 8,000-V DC voltage and 160-V pulsed voltage. Our inability to field evaporate boron carbide with voltage pulses can be attributed to its large band gap (the room temperature band gap of boron carbide is estimated to be 1.6–2.0 eV) (7).

The recent development of laser-assisted APT has made it possible to characterize a broader array of semiconductors and insulators. Like the traditional pulsed voltage approach, laser-assisted APT achieves 3D atomic-scale analysis by using a high electric field to remove individual atoms (or molecules) from material surfaces and a position-sensitive detector to determine their location and chemical identities. Thermal vibrations associated with rapid laser pulsing can displace a surface atom (or molecule) slightly away from the tip and cause its electrons to channel into the tip, resulting in a charged ion. After created, this ion is pulled off the surface and accelerated toward a detector by the intense electric field. The field evaporation experiments for this study were performed using a 355-nm UV laser-assisted atom probe (Cameca 4,000× Si). The laser illumination frequency was 250 kHz, and the laser dwell time was 8 ps per pulse. High DC voltages (4–8 kV depending on the specimen tip radii) were applied to generate an intense electric field. Altogether, six separate experiments were carried out—two with a 30-pJ laser pulse at 50 K, two with a 50-pJ laser pulse at 50 K, and two with a 30-pJ laser pulse at 20 K.

Field evaporation under laser illumination is thought to be a thermally assisted process with rapid temperature changes (31, 32). Previous investigations of laser-induced heating of atom probe tips have focused primarily on metals. The calculated temperature rises for tungsten and other metal tips were estimated to be ~300 K in normal experimental conditions (29) and up to ~800 K in extreme conditions (29, 33, 34). It is difficult to directly assess the tip temperature of laser-illuminated semiconductors and insulators, because the temperature in the specimen depends on its thermal diffusivity, thermal conductivity, specific heat, and density, all of which are temperature-dependent (35). There is, however, strong experimental evidence to

show that semiconducting GaAs nanowires remain crystalline during laser-assisted field evaporation experiments (36, 37). Du et al. (36, 37) performed atom probe experiments with laser energies (10–100 pJ) similar to those used in this study (30–50 pJ), and they obtained field desorption maps that revealed clear crystallographic poles, which indicate that the entire specimen, including the very surface atoms before evaporation, remained crystalline. The absence of melting indicates that the tip temperature stayed below the melting point of GaAs (1,511 K), which is about one-half of that for boron carbide (3,036 K). Inspired by these experiments on GaAs, we interrogated our boron carbide datasets and found the presence of lattice planes in the reconstructed volume (Fig. 3), confirming that no melting occurred on the atom probe tip surface in this study.

Moreover, the mass resolution is high in all experiments, and thermal tails were not severe, as shown in Fig. S2. The absence of severe thermal tails suggests that the thermal energy dissipates quickly so that there is no excessive heat building up between pulses.

Data Interpretation. It has been known to the atom probe community that APT tends to underestimate boron content in pure boron and boron-doped materials. Such underestimation is because boron tends to form multiple events, and because of the dead time of the detector, some B ions in the multiple events failed to be detected. Up to 36% loss of total boron signal in pure boron has been reported (38). In this work, we observed that, as the event multiplicity increases, the boron content decreases. Such decrease in boron detection is not associated with the multiple event-related detector dead time. If substantial boron signals were lost in the multiple events, it would have led to an overall underestimation of boron in B₄C. However, the measured stoichiometry by APT agrees well with the nominal composition. This consistency provides strong experimental evidence that the detected signals accurately reflect the chemistry of the field-evaporated species.

Moreover, the field-evaporated atoms and molecules captured by the detector provide spatial and chemical analyses of the liberated species. The *x–y* position of the ion on the detector provides spatial information, and the TOF of the ion points to its chemistry. The *z* position is determined by the order in which the atoms are detected. As atomic layers are field evaporated by successive laser pulses, the specimen becomes slightly blunter. Small increments in DC voltage are required to continue field evaporation.

In the simplest case, one pulse liberates a single ion from the specimen surface, and it is termed as a single event. In many ceramic systems, one laser pulse can release two or more ions from the specimen surface, and such an event is termed as a multiple event. It has generally been assumed that atoms in the multiple events were from random locations on the specimen surface. Recent studies by Müller et al. (39) and Yao et al. (40) showed the opposite—most of the atoms in each multiple event were spatially correlated. Analysis of the data obtained here also reveals a spatial correlation of the atoms in multiple events (an example is shown in Fig. S3). If the atoms from the same multiple event were randomly distributed, no peaks would be present in the histogram. The majority of atoms from the same pulse were less than 2 nm apart. The strong spatial correlation of the atoms in the multiple events suggests that they were released from the same site rather than from random locations and originally bonded together. The spacing is slightly larger than an icosahedron, because the positively charged atoms repel each other during the early stage of the

flight and their detected position deviated slightly from the original position.

Multiple events during field evaporation can take place in two scenarios. (i) The chemical bonds of a few atoms on the tip surface break in a correlated event. The liberated ions are accelerated and captured by the detector at the same time and recorded as a multiple event. (ii) A molecule is first field evaporated and then, accelerated toward the detector but decomposes into individual ions during the flight. On arriving at the detector, the decomposed ions are captured simultaneously and recorded as a multiple event. In this study, the multiple events associated with the field evaporation of boron carbide are most closely associated with the first scenario. That is to say that the detection of B and C ions for a single laser pulse results from individual B and C atoms being released from the specimen surface at the same time. If the second scenario was true (that is to say if molecules were evaporated and then decomposed during the flight), there would be a slight delay in the detection of the corresponding ions, because the molecule is heavier than the ions. Saxey (41) proposed that this delay would create distinctly curved tracks in the multiple event correlation histogram, and good examples of this can be found in figure 6 in ref. 41 and figure 6 in ref. 42. No such traces were observed in our Saxey plots of multiple event correlation histograms (Fig. S4). The absence of the traces indicates that in-flight decomposition of molecular ions did not occur in our boron carbide experiments and that the chemical bonds between individual atoms were broken before they left the specimen surface.

Ab Initio Simulation Methods. The quantum mechanics calculations were performed with the Vienna ab initio simulation package using the PBE functional and the projector augmented wave method to account for the core–valence interactions. A kinetic energy cutoff of 500 eV for the plane wave expansions was used. The convergence criteria were set to 1×10^{-4} eV energy difference for solving the electronic wave function and 1×10^{-2} eV/Å force for geometry optimization. Γ -Point sampling was used to sample Brillouin zone. Ab initio dynamical simulations were performed in the canonical ensembles (fixed number of atoms, fixed volume, and fixed temperature of the system) using Nosé thermostats (damping constant 100 fs) to control the temperatures. Newton's equations of motion were integrated using the Verlet algorithm with a time step of 2 fs.

The free surface was created from a perfect crystal. The crystal was constructed with a along [21–30], b along [01–10], and c along [0001] and 90 atoms per cell. We created the (0001) surface [(111) surface when viewed in rhombohedral symmetry] by a sequence of tensile deformation along the [0001] direction using a step of 0.02 strain. The atomic positions were optimized at each step. Dipole corrections and surface spin polarization were allowed in the slab simulations. We found that surface is created

at a 0.28 tensile strain. We annealed the surface from 800 to 300 K within 8 ps. We found that the icosahedra remain intact during these procedures. We used the same procedure to create the (100) surface. However, the icosahedra were already broken during the application of the tensile step. Because the APT experimental results do not depend on the crystal orientations, we chose a (111) surface for the field evaporation simulations, which is expected to be the most stable configuration for surface icosahedra.

Ejecting charged atoms in atom probe in the physical experiments consists of two steps: field ionization and field evaporation. Because the electron transfer dynamics is extremely challenging to simulate using density functional theory (DFT), we removed four electrons from the model to mimic the postionized state. Then, we applied a very strong electric field along with thermal perturbations to emulate the thermally assisted field evaporation process. The value of 30 V/Å was used as the electric field strength, comparable with the experimental estimation (28). Thermal perturbation was introduced by heating the charged model from 300 to 2,050 K within 8 ps to interrogate which bonds are broken and which possible species can be released from the system. Note that, because of the extremely small size of simulation cell and the extreme high heating rate of 2.2×10^{14} K/s, we need to go to much higher temperature in simulations to observe the key processes of bond breaking and icosahedra deconstruction. Thus, the temperature to kindle field evaporation in the simulation is much higher than the physical experiments. It is also worth mentioning that the melting point of boron carbide is 3,036 K. Even at a temperature as high as 2,000 K, no melting should have occurred. The destruction of the icosahedra in the simulation is purely attributed to the interplay of strong electric field and thermal perturbation rather than melting—same as the experimental observation.

To gain quantitative insight on the relative stabilities of the surface chain vs. icosahedra, we computed the minimum energy (E) to extract the B-C from the chain and the icosahedron in the slab model (Fig. S5). The minimum energy is described as

$$E = E_{slab-BC} + E_{BC} - E_{slab},$$

where E is the minimum extraction energy, $E_{slab-BC}$ is the slab energy after extracting B-C from chain or icosahedron, E_{BC} is energy of the B-C diatomic cluster, and E_{slab} is slab energy before extracting the B-C cluster.

The minimum energy is 9.18 eV to extract the B-C from the icosahedron, whereas it requires 12.15 eV to extract the B-C from the chain structure. The results indicate that the B-C in the icosahedra is less stable than that in the chains.

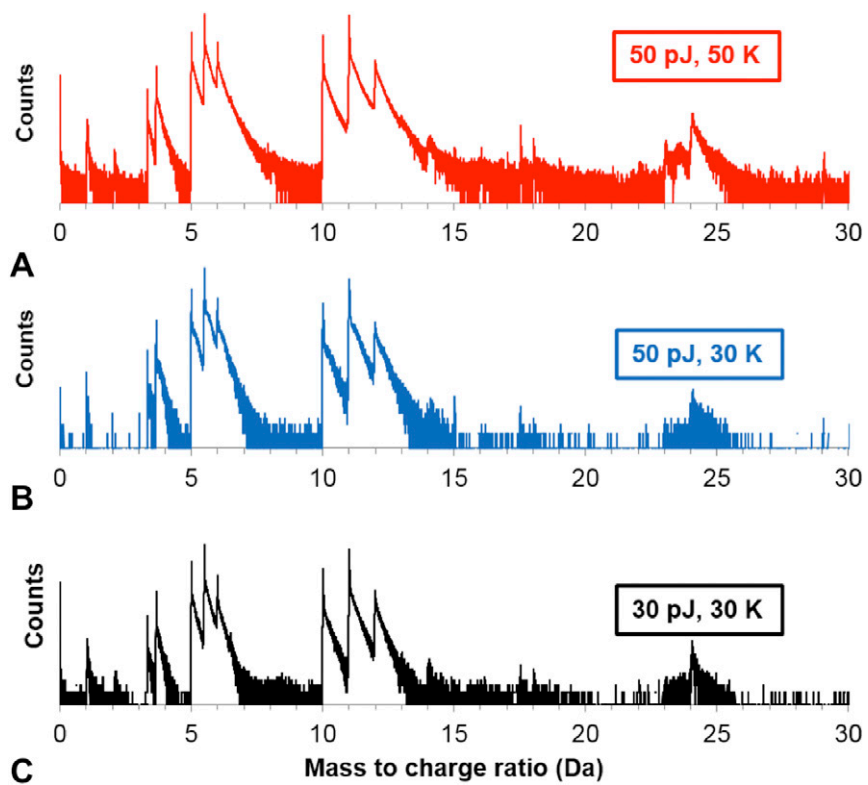


Fig. S2. Mass spectra of boron carbide field evaporated at (A) 50 pJ and 50 K, (B) 50 pJ and 30 K, and (C) 30 pJ and 30 K. Note that the y axis is in log scale and that none of the datasets have severe thermal tails that would be an indication of excessive heating.

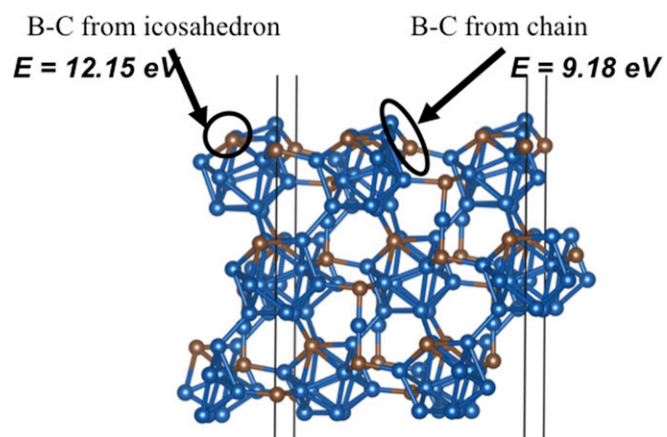
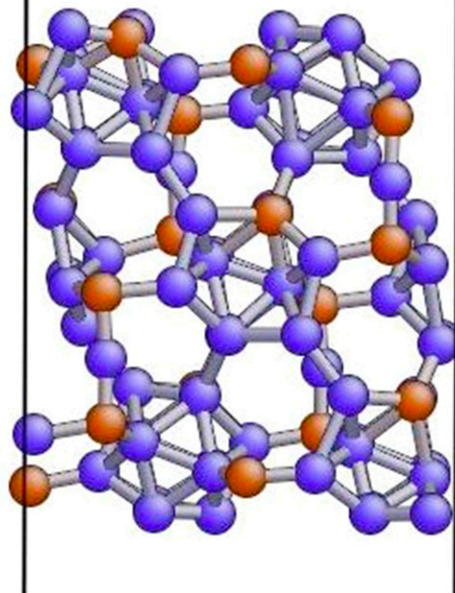


Fig. S5. QM simulation model showing the locations of B-C diatomic clusters from the chain and icosahedron. The removal of each increases the overall system energy, and such energy was used to quantify the stability of chains and icosahedra in boron carbide.

300.0



Movie S1. Ab initio simulation of field evaporation of boron carbide with a (111) free surface from 300 to 2,050 K.

[Movie S1](#)